JOURNAL OF THE KOREAN ASTRONOMICAL SOCIETY
29: 181~194, 1996

WASHINGTON CCD PHOTOMETRY OF THE OLD OPEN CLUSTER NGC 1245

WEE, SUN- OK AND LEE, MYUNG GYOON
Department of Astronomy, Seoul National University
e-mail: wesun@astro.snu.ac.kr, mglee@astrog.snu.ac.kr
(Received September 25, 1996; Accepted October 15, 1996)

ABSTRACT

We present a study of the metallicity of the old open cluster NGC 1245 , based on the Washington CCD photometry obtained using the 0.6 m telescope at the Sobaeksan Observatory, Korea. NGC 1245 has been known to be a unique cluster among the known open clusters in the sense that the previous metallicity estimates for this cluster are much larger (by 3σ) than the value expected from the radial metallicity gradient of the old open clusters in Our galaxy. We have estimated the metallicity of the cluster red giants using the four color-color diagrams, obtaining a value for the mean metallicity of [Fe/H] $= -0.04 \pm 0.05$ dex. The total error including the error of the metallicity calibration, 0.15 dex, is 0.16 dex. The metallicity estimate of NGC 1245 we have obtained in this study is smaller than previous estimates, and is consistent with the radial metallicity gradient of the old open clusters, showing that the mean metallicity of NGC 1245 is not abnormally high. The reddening, distance, and age of the cluster have also been derived using the isochrones based on the convective overshooting models: the reddening $E(B-V) = 0.28 \pm 0.03$; the distance $d = 2.5 \pm 0.2$ kpc (the corresponding galactocentric distance is $R_{GC} = 10.7$ kpc, and the distance from the galactic plane is $z = -0.4$ kpc); and the age $t = 1.1 \pm 0.1$ Gyrs.

Key Words: open clusters: NGC 1245 — HR diagram — Galaxy: abundance, evolution

I. INTRODUCTION

Old open clusters provide us with an important information on the early evolution of the Galactic disk. There are about 70 known old open clusters with ages > 1 Gyrs (Friel 1995). These clusters are in general faint. With the advent of CCD camera in astronomy, the number of studies on these clusters has been increasing. However, there are still many of these clusters for which basic parameters are not known. For example, metallicities of about 30 clusters among these clusters are not yet known.

NGC 1245 is one of the old open clusters for which the metallicity is not well-known. NGC 1245 (C0311+470) is an irregular loose open cluster located in the antigalactic direction ($\alpha(1950) = 3^h11^m.2$, $\delta(1950) = 47°4'$, $l = 146°.6$, $b = -8°.9$). According to the recent summary of the properties of the old open clusters (Friel 1995), the metallicity of NGC 1245 is [Fe/H] = +0.14 dex (Lynga 1987). This value of the metallicity is the second highest among the metallicities of the known old open clusters (the highest one is the metallicity of NGC 6791, [Fe/H] = +0.15 dex). This value is much larger (by 3σ level) than that expected at the distance of NGC 1245 (about 11 kpc) from the relation of the metallicity and the galactocentric distance for the old open clusters (see Fig. 7 in Friel (1995)). NGC 1245 shows the largest deviation in the relation of the metallicity and the galactocentric distance for the old open clusters

It is intriguing that NGC 1245 has such a metallicity, considering the distance of the cluster in the galactic disk. There are two possibilities for this intriguing problem: the intrinsic metallicity of NGC 1245 is abnormally high for some reasons; or the previous estimates of the metallicity of NGC 1245 may be overestimates.

We have carried out a photometric study of NGC 1245 to resolve this problem, which is presented in this paper.

We have estimated the metallicity of NGC 1245 using Washington CCD photometry which is accurate and efficient for determining the metallicity of late type stars (Canterna 1976, Geisler *et al.*1991). This paper is composed as follows. Sec.II presents observations and data reduction, Sec. III shows the color-magnitude diagrams, and Sec. IV estimates the metallicity, reddening, distance and age. Sec. V discusses the differential reddening of NGC 1245 and the radial metallicity gradient of the old open clusters. Finally, summary and conclusions are given in Sec. VI.

Table 1. Observational Log of NGC 1245

Area	Filter	Exposure Time	Observation Time(UT)	Airmass	Seeing
W-field	C	3× 150 sec	$11^h\ 17^m$	1.158	4.″2
W-field	M	3× 120 sec	$11^h\ 08^m$	1.140	4.″0
W-field	T_1	3× 90 sec	$11^h\ 00^m$	1.125	3.″6
W-field	T_2	3× 70 sec	$10^h\ 48^m$	1.109	3.″9
E-field	C	3× 150 sec	$11^h\ 33^m$	1.190	3.″9
E-field	M	3× 120 sec	$11^h\ 56^m$	1.251	3.″9
E-field	T_1	3× 90 sec	$12^h\ 05^m$	1.274	3.″8
E-field	T_2	3× 70 sec	$12^h\ 20^m$	1.324	3.″5

II. OBSERVATIONS AND DATA REDUCTION

(a) Observations

The CMT_1T_2 CCD images of NGC 1245 were obtained using the Photometrics PM 512 CCD camera and the 0.6 m telescope at Sobaeksan Observatory, Korea, on the photometric night of February 19, 1996. The pixel scale is 0.″5 per pixel and the size of the CCD field is 4.′3 × 4.′3. NGC 1245 (15′ × 15′) is much larger than the size of a CCD field so that we observed two central regions in NGC 1245: called as E-field and W-field, respectively. Our CCD fields are overlapped mostly with the field studied by Carraro & Patat (1994). The observing log is given in Table 1. There were strong wind on the night of observation so that the seeing was rather poor, 4.0 arcsec. However, our target stars are bright and there is little crowding in NGC 1245 so that we could secure good photometry of the bright stars in NGC 1245. Figure 1 displays the regions of NGC 1245 we observed.

(b) Data Reduction

The instrumental magnitudes of NGC 1245 were obtained using IRAF/DAOPHOT. The resulting instrumental magnitudes were transformed onto the standard system using the standard stars observed on the the same night (Geisler 1990, 1996).

The transformation equations to the standard system are :

$$T_1 = t_1 - 0.141(m - t_1) - 0.064X - 6.909,$$

$$(C - M) = 1.129(c - m) - 0.356X - 0.593,$$

$$(T_1 - T_2) = 0.858(t_1 - t_2) - 0.024X - 0.447, \text{ and}$$

$$(C - T_1) = 1.162(c - t_1) - 0.386X + 0.386,$$

where the lower symbols represent the instrumental magnitudes and the upper symbols represent the standard magnitudes. The zero point of the instrumental magnitudes were arbitrarily set to be 25.0. The calibration errors are 0.02–0.03 mag for the magnitudes and colors.

We have measured 248 stars in total. Table 2 lists the photometry of the 187 stars brighter than $T_1 = 16.5$ mag, and Table 3 presents the mean photometric errors versus T_1 magnitudes.

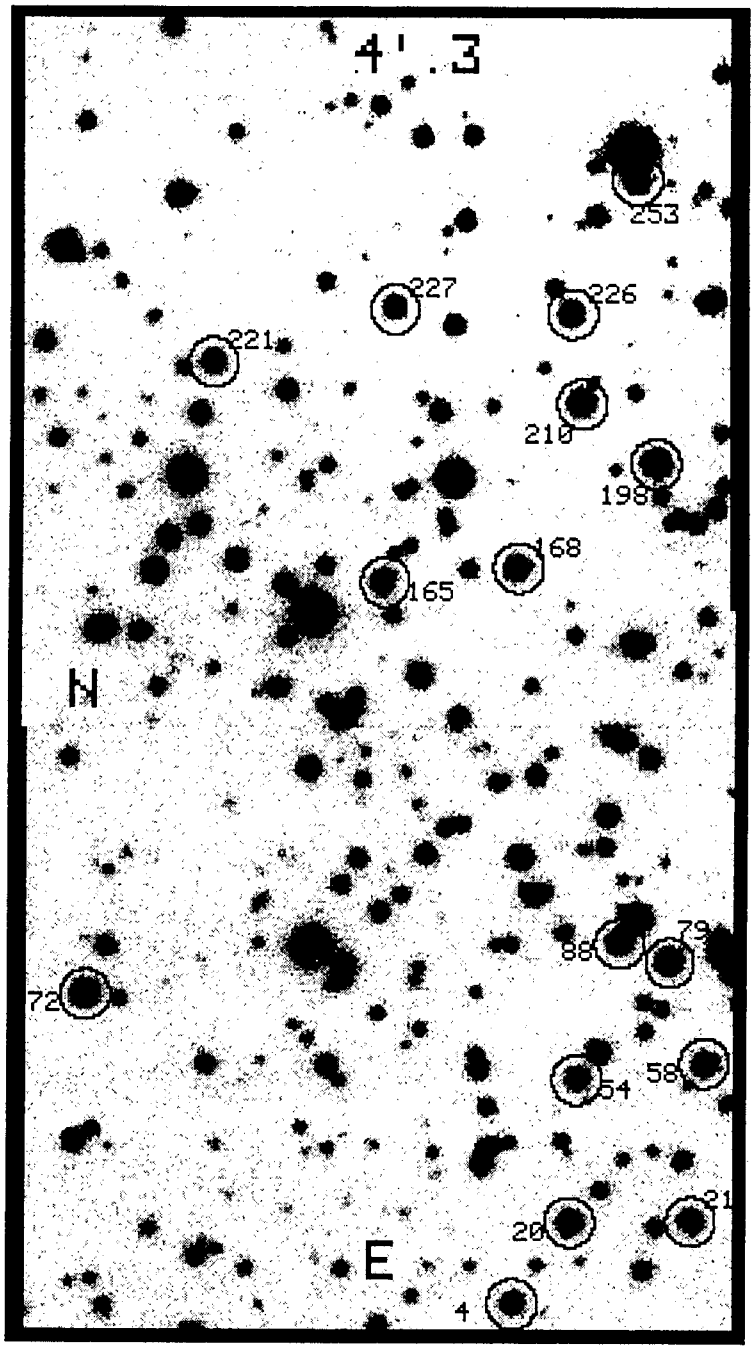

Fig. 1 A greyscale map of the T_1 CCD images of the central $8'.0 \times 4'.3$ region of NGC 1245. West is up and north is to the left. The circles represent the bright red giant stars used for the metallicity estimates.

(c) Comparison with Previous Photometry

Only a few sets of photometry of NGC 1245 were published before this study. Hoag *et al.*(1961) presented UBV photometry of about 200 bright stars; Chincarini (1964) presented UBV photoelectric and photographic photometry of 500 stars including Hoag *et al.*(1961)'s; and recently Carraro & Patat (1994) presented deep BV CCD photometry.

We have transformed T_1 magnitudes and $(C - T_1)$ colors into V magnitudes and $(B - V)$ colors using the transformation equations given by Geisler (1996): $(B - V)_{(C-T_1)} = 0.076 + 0.475(C - T_1)$, and $V_{T_1} = 0.052 + T_1 + 0.256(C - T_1)$. Then we have compared these transformed V_{T_1} magnitudes and $(B - V)_{(C-T_1)}$ colors with those of

Table 2. Photometry of the bright stars ($T_1 \leq 15$ mag) in NGC 1245.

Star	X	Y	T_1	$(C-M)$	(T_1-T_2)	$(C-T_1)$	Star	X	Y	T_1	$(C-M)$	(T_1-T_2)	$(C-T_1)$
2	229.3	8.8	15.27	0.82	0.52	1.46	88	41.6	140.2	13.23	1.34	0.62	2.26
4	79.6	10.0	13.62	1.37	0.64	2.35	89	5.1	140.8	13.59	1.38	0.67	2.32
5	116.5	12.4	15.83	0.65	0.42	1.27	91	61.8	143.4	15.12	0.55	0.32	1.00
7	233.9	18.5	16.16	0.70	0.51	1.34	92	35.7	148.9	12.63	0.38	0.22	0.63
8	33.1	21.7	14.62	0.64	0.39	1.17	93	129.2	151.3	14.53	0.61	0.38	1.07
9	143.0	22.3	15.39	0.76	0.42	1.30	95	172.3	155.4	16.43	0.77	0.57	1.29
10	177.6	22.6	15.68	1.14	0.64	2.05	96	121.1	157.4	15.08	0.61	0.41	1.06
11	95.2	23.1	16.43	0.96	0.48	1.59	97	72.8	157.4	13.83	0.58	0.31	0.96
13	71.3	23.7	15.99	1.28	0.76	2.24	98	68.8	158.6	15.49	0.62	0.43	1.10
15	195.9	26.8	14.42	0.97	0.52	1.69	100	143.7	161.2	14.88	0.64	0.43	1.11
16	188.3	29.4	16.40	0.54	0.50	1.25	101	40.6	162.8	16.30	0.64	0.32	1.35
18	212.8	36.8	15.44	0.69	0.42	1.19	103	228.2	166.3	16.17	0.68	0.51	1.26
19	28.1	37.4	14.80	0.62	0.32	1.05	107	137.5	170.7	14.63	0.61	0.34	1.04
20	59.2	39.3	13.25	1.30	0.64	2.24	108	77.6	171.2	13.48	0.55	0.25	0.90
21	15.4	40.0	13.54	1.57	0.73	2.63	109	112.3	172.1	14.24	0.64	0.36	1.11
26	48.4	50.9	15.18	0.57	0.34	1.03	112	54.5	174.2	16.24	0.81	0.55	1.56
27	90.8	60.0	13.93	0.71	0.42	1.23	113	47.1	175.2	14.89	0.60	0.40	1.08
29	18.6	61.5	14.64	0.55	0.32	0.92	114	104.9	182.0	14.97	0.66	0.36	1.09
30	39.9	62.2	16.02	0.69	0.42	1.31	115	98.9	183.6	15.14	0.67	0.35	1.21
32	108.8	64.1	15.98	0.66	0.43	1.26	117	46.3	186.8	13.75	0.60	0.33	1.05
34	29.2	64.8	16.18	0.68	0.45	1.25	121	86.4	198.6	14.96	0.60	0.34	1.01
35	148.0	65.5	16.05	0.69	0.45	1.38	122	135.9	199.7	15.22	0.66	0.43	1.13
37	89.5	66.2	14.90	0.65	0.38	1.11	124	72.3	201.1	14.22	1.02	0.49	1.75
38	85.5	66.8	15.81	0.84	0.59	1.53	125	119.7	202.5	16.35	0.75	0.52	1.30
41	240.4	67.9	14.02	0.71	0.43	1.24	126	155.4	203.7	13.69	0.99	0.55	1.79
42	80.8	68.1	15.94	1.29	0.50	2.33	128	242.5	207.4	14.85	0.63	0.38	1.06
43	62.2	68.3	15.41	0.66	0.38	1.19	129	31.2	207.6	14.08	0.55	0.31	0.92
45	233.8	72.3	15.52	0.69	0.47	1.19	130	66.7	209.4	16.03	0.74	0.43	1.25
46	157.7	73.3	16.07	0.74	0.50	1.29	134	40.6	213.7	13.97	0.57	0.33	0.94
48	89.2	80.2	14.96	1.38	0.72	2.37	135	45.0	215.3	14.27	0.61	0.31	1.01
49	2.4	81.7	15.22	0.64	0.37	1.16	138	101.1	221.5	14.07	0.62	0.31	1.06
52	16.4	88.5	16.27	0.71	0.49	1.35	139	144.2	222.7	12.77	1.03	0.57	1.80
53	144.0	89.7	15.88	0.64	0.42	1.21	140	137.9	225.4	16.45	0.81	0.60	1.45
54	56.5	91.0	13.69	1.36	0.63	2.32	141	150.3	226.9	15.09	0.67	0.44	1.23
55	92.2	94.2	14.44	0.63	0.36	1.06	142	139.2	230.0	15.21	0.72	0.43	1.26
56	148.5	95.4	14.23	0.65	0.33	1.06	144	167.2	232.3	14.51	0.97	0.51	1.72
57	192.5	95.6	14.77	0.63	0.38	1.10	145	211.6	232.6	15.10	0.62	0.39	1.05
58	10.6	96.0	13.30	1.33	0.62	2.29	147	74.8	233.4	15.64	0.66	0.46	1.29
61	93.6	99.5	15.70	0.66	0.38	1.19	148	115.5	236.8	13.41	0.65	0.34	1.11
62	49.2	100.2	13.81	0.60	0.34	1.02	150	191.5	239.7	15.90	0.66	0.46	1.24
64	155.5	105.1	16.36	0.81	0.59	1.49	151	37.9	248.5	13.13	0.24	0.19	0.45
65	32.4	107.7	15.30	0.55	0.33	1.01	153	164.7	251.1	14.19	0.65	0.34	1.16
66	113.8	108.4	15.89	0.84	0.50	1.46	154	59.3	251.6	15.15	0.61	0.33	1.08
68	130.0	114.3	15.55	0.59	0.47	1.23	156	233.6	253.4	13.40	1.24	0.64	2.15
69	26.3	115.8	15.47	0.76	0.44	1.34	157	230.6	254.0	14.00	0.65	0.38	1.22
70	33.0	118.4	15.46	0.71	0.40	1.24	158	11.7	258.6	15.02	0.58	0.32	1.03
71	224.3	119.3	15.50	0.73	0.42	1.24	159	125.9	259.4	14.82	0.61	0.40	1.06
72	236.3	121.3	12.69	1.71	0.73	2.81	160	154.9	259.4	10.68	1.60	0.70	2.65
73	93.6	121.7	16.19	0.81	0.45	1.47	161	184.9	261.3	16.33	0.74	0.58	1.32
74	146.3	123.9	16.35	0.36	0.69	0.87	162	161.8	266.5	16.05	0.77	0.23	1.74
75	115.8	126.0	16.16	1.15	0.62	1.77	164	165.6	270.1	14.00	0.59	0.32	1.05
76	142.4	126.6	14.46	0.67	0.37	1.13	165	129.8	271.0	13.28	1.39	0.65	2.35
77	114.3	130.8	16.02	1.32	0.72	2.33	166	213.1	275.0	13.17	1.10	0.59	1.91
78	142.3	132.2	13.85	0.63	0.31	1.04	167	97.8	275.4	14.76	0.61	0.39	1.08
79	23.9	132.9	12.92	1.40	0.63	2.37	168	80.5	276.0	13.27	1.38	0.64	2.33
81	5.3	135.6	14.07	0.87	0.39	1.11	169	150.7	276.8	14.81	0.69	0.41	1.27
83	154.2	138.0	10.91	0.76	0.43	1.33	171	183.4	278.8	13.94	0.64	0.38	1.10
84	229.0	138.5	14.52	0.71	0.42	1.22	172	125.5	281.1	15.89	0.90	0.59	1.58
85	85.9	139.1	15.81	0.68	0.41	1.19	174	119.3	283.7	15.32	0.68	0.47	1.16
86	81.0	139.4	15.44	0.66	0.39	1.10	175	207.9	286.7	13.70	0.68	0.43	1.22

Table 2. (Continued)

Star	X	Y	T_1	$(C-M)$	(T_1-T_2)	$(C-T_1)$	Star	X	Y	T_1	$(C-M)$	(T_1-T_2)	$(C-T_1)$
178	196.9	291.4	13.94	0.58	0.33	1.00	221	191.9	350.8	13.44	1.42	0.66	2.39
179	15.6	292.2	14.64	0.64	0.34	1.21	222	166.4	356.1	15.58	0.70	0.45	1.28
180	25.2	292.6	15.42	1.54	0.61	2.61	223	253.1	357.9	14.02	1.28	0.63	2.26
181	21.7	294.0	15.18	0.61	0.42	1.08	224	103.1	364.1	13.98	0.61	0.34	1.05
182	106.6	294.3	15.39	0.83	0.55	1.53	225	213.4	367.0	15.92	1.38	0.75	2.30
183	8.3	297.8	14.33	0.52	0.25	0.89	226	60.9	368.2	13.23	1.40	0.64	2.35
185	28.6	302.0	14.97	0.53	0.29	0.99	227	125.3	370.7	13.58	1.39	0.65	2.37
186	223.8	303.3	15.59	0.69	0.43	1.23	228	12.3	372.5	14.32	0.53	0.33	0.97
187	122.5	303.5	15.44	1.40	0.73	2.36	229	8.4	373.1	14.09	0.91	0.48	1.64
189	118.6	305.1	15.90	0.68	0.48	1.33	231	66.7	377.4	14.77	0.57	0.33	0.99
190	157.8	305.4	16.37	0.60	0.53	1.35	232	225.3	379.6	15.80	0.60	0.45	1.22
191	5.7	305.8	14.96	0.55	0.36	0.95	233	150.6	379.7	14.80	1.02	0.56	1.79
193	103.4	308.3	11.59	1.13	0.49	1.90	237	241.5	389.1	15.13	0.65	0.38	1.20
194	157.7	308.9	15.96	0.96	0.53	1.60	238	232.9	390.4	15.56	0.63	0.43	1.19
195	201.7	309.2	11.33	2.28	1.77	3.83	240	246.7	392.1	12.70	1.23	0.54	2.08
196	44.6	311.6	16.18	0.77	0.39	1.37	243	105.6	397.9	16.25	0.57	0.38	1.32
197	149.9	312.9	15.34	0.62	0.41	1.13	245	98.8	401.9	14.17	0.85	0.46	1.52
198	30.1	313.9	12.52	1.57	0.70	2.60	246	51.6	403.8	14.16	1.55	0.72	2.65
200	168.5	316.1	16.34	0.91	0.62	1.56	249	204.6	411.0	13.37	0.62	0.35	1.06
202	218.6	322.3	15.67	0.70	0.47	1.30	251	12.6	412.8	15.61	0.68	0.36	1.24
203	248.1	322.7	14.73	0.57	0.35	1.00	253	37.2	416.1	13.55	1.32	0.62	2.28
204	6.3	324.9	15.11	0.71	0.30	1.19	255	52.0	421.6	15.25	0.67	0.25	1.39
207	196.8	331.6	13.90	0.33	0.20	0.55	256	39.1	427.2	10.26	2.15	0.92	3.57
208	108.3	332.6	13.91	0.81	0.46	1.44	257	114.8	432.0	14.28	0.72	0.45	1.32
209	88.9	334.5	15.76	0.60	0.46	1.14	258	96.3	432.6	14.63	0.57	0.34	0.94
210	57.2	336.0	12.95	1.41	0.65	2.39	259	183.6	433.8	15.31	0.61	0.35	1.09
212	114.9	337.7	16.24	0.79	0.52	1.39	260	238.5	437.3	14.93	0.58	0.38	1.01
213	254.9	337.9	16.10	0.82	0.55	1.34	263	131.0	443.3	14.76	0.62	0.36	1.09
215	37.7	339.6	15.21	0.65	0.39	1.11	264	141.6	445.3	16.10	0.68	0.39	1.41
216	165.0	340.4	13.93	0.74	0.45	1.31	265	120.5	451.7	15.66	1.48	0.69	2.38
217	142.1	341.0	15.96	0.82	0.56	1.53	266	6.4	455.1	14.64	0.56	0.28	1.04
218	52.4	343.5	16.22	0.85	0.42	1.56	269	151.0	472.0	16.16	0.82	0.54	1.39
219	70.3	348.6	16.19	0.66	0.42	1.32	271	206.9	472.4	13.85	0.70	0.42	1.26
220	202.9	348.6	15.29	0.72	0.47	1.35							

Table 3. Mean photometric errors versus T_1 magnitude of NGC 1245

T_1	$\sigma(T_1)$	$\sigma(C-M)$	$\sigma(T_1-T_2)$	$\sigma(C-T_1)$	$\sigma(M-T_2)$
12.5	0.005	0.008	0.007	0.009	0.006
13.5	0.008	0.014	0.012	0.015	0.010
14.5	0.012	0.021	0.017	0.021	0.016
15.5	0.022	0.043	0.028	0.047	0.023
16.5	0.047	0.100	0.057	0.107	0.044
17.5	0.099	0.244	0.117	0.254	0.094

Chincarini (1964) and Carraro & Patat (1994). The number of stars common in ours and Chincarini's photometry is 120, and the number of stars common in ours and Carraro & Patat's photometry is 185.

Figure 2 shows the comparison of our photometry and those by Chincarini (1964) and Carraro & Patat (1994). Figures 2(a) and (b) show that there is a significant non-linearity in the photographic V magnitudes in Chincarini's photometry and that our colors are systematically redder than Chincarini's. The mean difference in the colors for 35 bright stars with $V < 15$ mag is $\Delta(B-V)$(This study–Chincarini 1964) $= 0.07 \pm 0.12$. Figures 2(c) and (d) show that our V magnitudes are systematically brighter than Carraro & Patat's and that our $(B-V)$ colors are, on average, bluer than Carraro & Patat's. The mean differences for the 56 bright stars with $V < 15$ mag are $\Delta(V)$(This study–Carraro & Patat 1994) $= -0.22 \pm 0.06$ and $\Delta(B-V)$(This study–Carraro & Patat 1994) $= -0.04 \pm 0.11$.

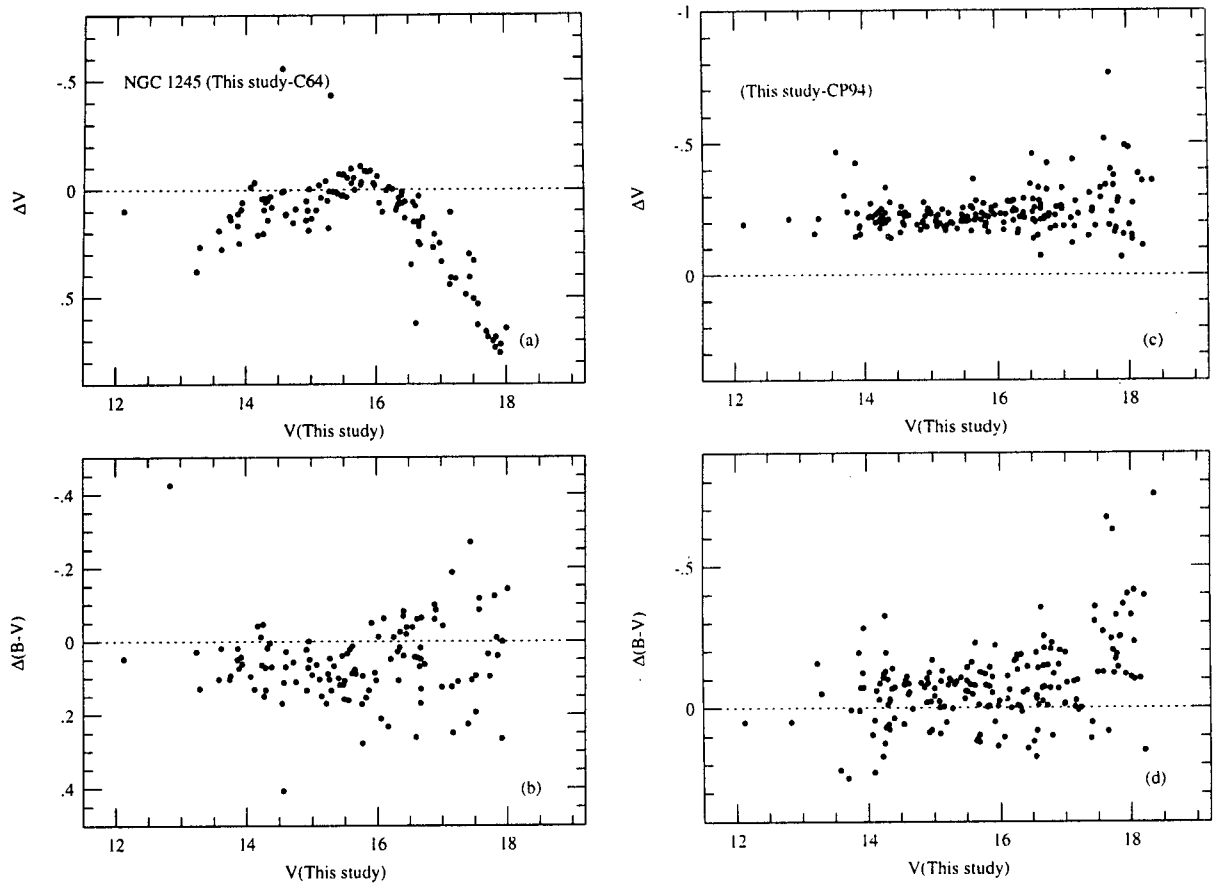

Fig. 2 Comparison of our photometry with those by Chincarini (1964) (a, b) and Carraro & Patat (1994) (c, d). The vertical axes represent the differences of V and $(B - V)$ in the sense ours minus others.

In summary, our colors and magnitudes for the bright stars are intermediate between Chincarini's and Carraro & Patat's.

We have plotted the $V - (B - V)$ color magnitude diagrams of the stars common among this study, Chincarini (1964) and Carraro & Patat (1994) on the same scale in Figure 3 to show the overall differences clearly. Main conclusions drawn from the inspection of Figure 3 are as follows. (1) The main sequence of this study is narrower than those of Chincarini's and Carraro & Patat's. (2) The general morphology of the red giant clump of this study is similar to Chincarini's, but the red giant clump of this study is much more concentrated than Carraro & Patat's. It is suspected that the photometry of Carraro & Patat might have suffered from some calibration problems. This point will be discussed further in Sec. 5.

III. COLOR-MAGNITUDE DIAGRAM OF NGC 1245

Figure 3 displays the $T_1 - (C - T_1)$ color-magnitude diagram of the ≈260 measured stars. The color-magnitude diagram of NGC 1245 is, in general, similar to other old open clusters. The main features seen in Figure 3 are as follows: (a) There is a broad main sequence the top of which is located at $T_1 \approx 13.8$ mag and $(C - T_1) \approx 1.1$ (corresponding to $V \approx 14.1$ mag and $(B - V) \approx 0.6$). (b) There are a group of red giant clump stars located at $T_1 = 13.5$ mag and $(C - T_1) = 2.3$ (corresponding to $V \approx 14.1$ mag and $(B - V) \approx 1.2$), which is seen typically in old open clusters. (c) There are a small number of stars scattered over the color-magnitude diagram, which are probably the non-members of the cluster.

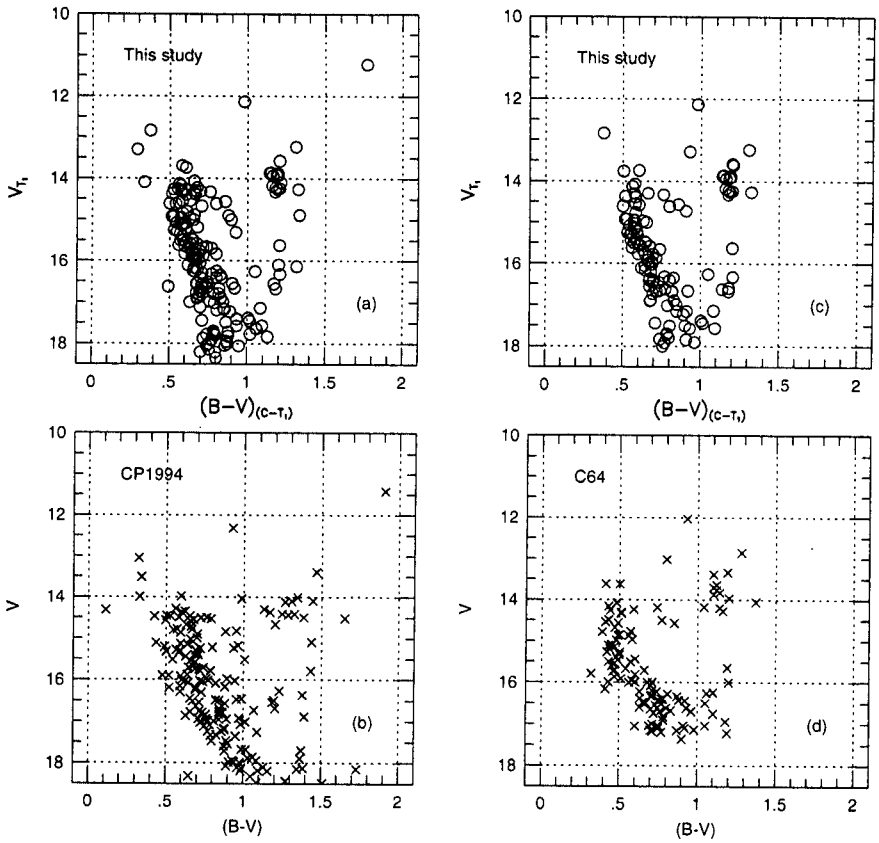

Fig. 3 Comparison of the $V-(B-V)$ color-magnitude diagrams of this study, Chincarini (1964), and Carraro & Patat (1994) on the same scale. (a) and (b) represent the stars common between this study and Carraro & Patat, and (c) and (d) represent the stars common between this study and Chincarini.

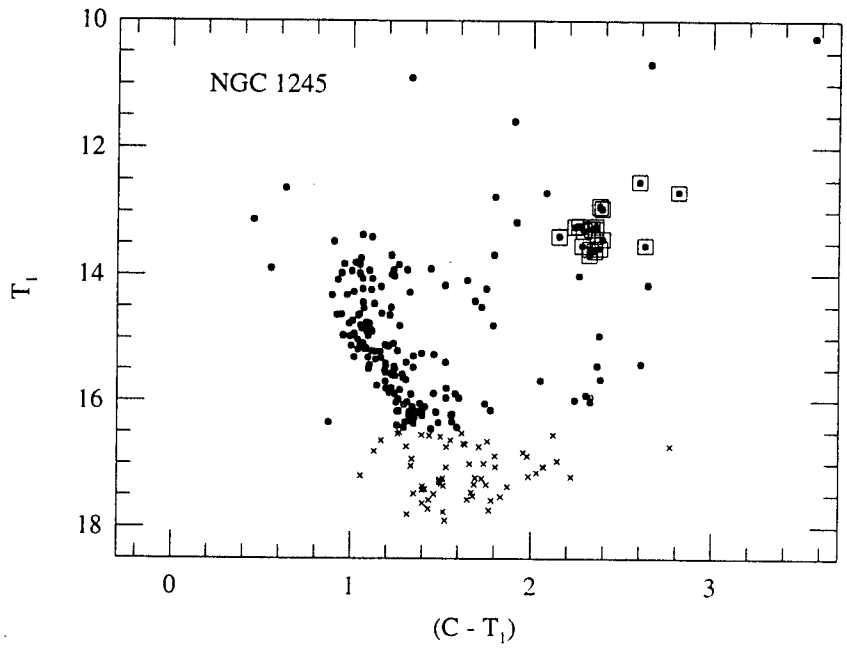

Fig. 4 $T_1-(C-T_1)$ color-magnitude diagram of NGC 1245. The filled circles represent the stars with small errors, and the crosses represent the stars with large errors. The squares represent the red giant stars used for estimation of the metallicity in this study.

IV. METALLICITY, REDDENING, AGE, AND DISTANCE

(a) The Method

The metallicity of late-type stars can be estimated using the color-color diagrams of Washington photometry which is described in detail in Geisler *et al.*(1991). We have to know the reddening first for using this method. However, the reddening for NGC 1245 is not yet well determined. So we have estimated the metallicity, reddening, distance and age of NGC 1245 using an iterative method explained as follows: (1) We choose red giant stars with small photometric errors. Inspecting the color-magnitude diagram shown in Figure 4, we have selected 16 red giant stars with $2.1 < (C - T_1) < 2.9$, $12.5 < T_1 < 13.8$ mag and photometric errors smaller than 0.02. These red giant stars were marked by the squares in Figure 4; (2) We assume initially a value for the reddening; (3) We estimate the metallicity using the color-color diagrams of the selected giants for the assumed reddening; (4) We choose theoretical isochrones for the estimated metallicity and a proper range of ages; (5) Then we perform fitting the main sequence of the cluster in the the color-magnitude diagram with the theoretical isochrones to obtain the distance and age of the cluster for the assumed reddening. We have used the $V - (B - V)$ color-magnitude diagram of NGC 1245 converted from Figure 3 using the procedures explained in Sec. 2, because the theoretical isochrones are not available in the Washington system at the moment; and (6) If the fitting is not suitable for the selected isochrones, we change the value of the assumed reddening and iterate the steps in (3) to (5) until the fitting is satisfactory. If the fitting is satisfactory, we obtain the reddening, metallicity, distance and age of the cluster all together.

(b) The Results

We have obtained a value of the reddening, $E(B - V) = 0.28 \pm 0.03$ following the method described above. The corresponding reddening values for other colors are $E(C - T_1) = 0.55$, $E(T_1 - T_2) = 0.19$, $E(C - M) = 0.30$, and $E(M - T_2) = 0.45$ (Harris & Canterna 1979, Geisler *et al.*1991).

Figure 5 shows four kinds of color-color diagrams of the Washington system for 16 selected red giant stars. The isoabundance lines in the color-color diagram given by Geisler *et al.*(1991) are plotted by the solid lines. We have used $(T_1 - T_2)$ and $(M - T_2)$ colors as a temperature index and $(C - M)$ and $(C - T_1)$ colors as a metallicity index. The colors are dereddened according to the reddening values given above. We have estimated the metallicities of the red giants using the four color-color diagrams in Figure 5, the results of which are listed in Table 4. The four estimates agree very well with a mean value of [Fe/H] $= -0.04 \pm 0.05$ dex. The mean dispersion of each estimate is Δ[Fe/H] $= \pm 0.14 \pm 0.02$ dex. The error in the calibration of this method is smaller than 0.15 dex (Geisler *et al.*1991) so that the total error of the mean metallicity is estimated to be smaller than 0.16 dex.

Figure 6 shows the isochrone fitting in the color-magnitude diagram of NGC 1245. We have used the theoretical isochrones based on the convective overshooting models given by the Padova group (Bertelli *et al.*1994). The main sequence of NGC 1245 is well matched by the isochrones for the metallicity of [Fe/H] = –0.04 dex and the age of 1.1 Gyrs which are shown by the solid line in Figure 6. The age of NGC 1245 is estimated to be $t = 1.1 \pm 0.1$ Gyrs.

The main sequence fitting yields a value for the distance modulus of NGC 1245, $(m - M)_V = 12.92 \pm 0.15$. The intrinsic distance modulus is $(m - M)_0 = 12.00 \pm 0.15$, which corresponds to a distance of $d = 2.5 \pm 0.2$ kpc. From this value we derive the galactocentric distance $R_{GC} = 10.7$ kpc and the distance from the galactic plane $z = -0.4$ kpc for the distance of the Galactic center, $R_0 = 8.5$ kpc.

(c) Comparison with Previous Studies

We have compared our estimates for the reddening, metallicity, age and distance of NGC 1245 with previous estimates in Table 5.

Our reddening estimate agrees very well with that given by Hagen (1970) who used UBV photometry, $E(B-V) = 0.27$. Our metallicity estimate is somewhat smaller than the values given by Janes (1979) and Lynga (1987). Janes (1979) estimated the mean metallicity of NGC 1245 using the UBV photometry given by Hagen *et al.*(1970).

Carraro & Patat (1994) obtained the reddening, $E(B - V) = 0.26$, and the distance, $d = 3.0$ kpc, and the age, $t = 0.8$ Gyrs, assuming the metallicity value of [Fe/H] = + 0.14 given in the Lund Catalog of Open Cluster Data

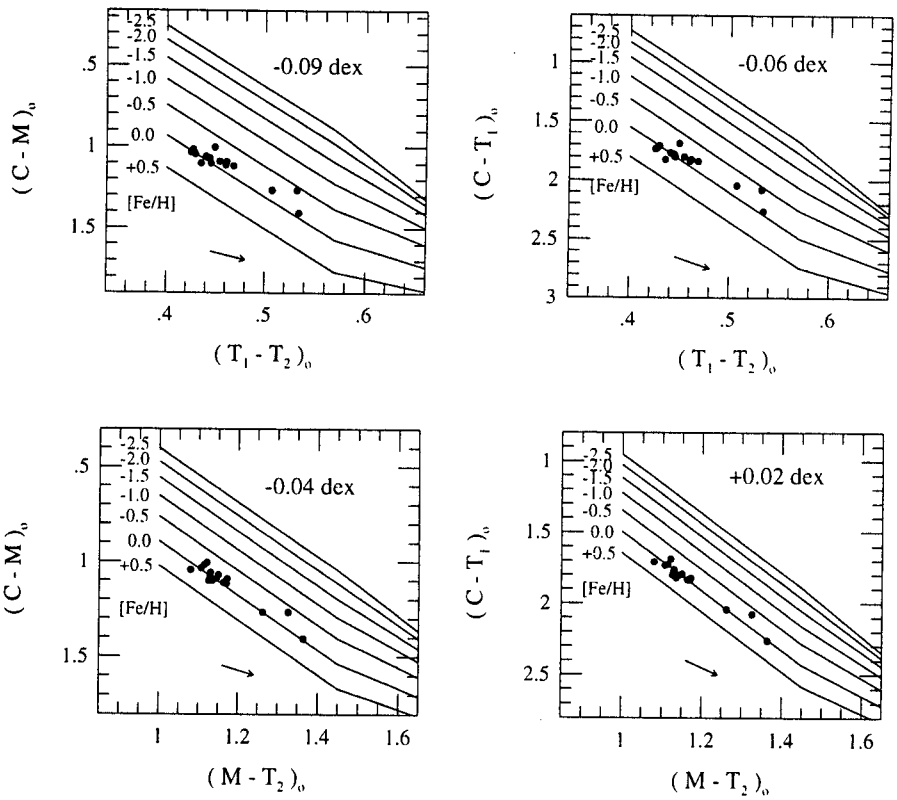

Fig. 5 Color-color diagrams of the red giant stars in NGC 1245. The solid lines represent isoabundance lines and the numbers at the left end of the solid lines are metallicity values. The short arrow lines at the lower part of each diagram represent the reddening direction. The numbers at the upper right part of each diagram represent the mean metallicity estimate.

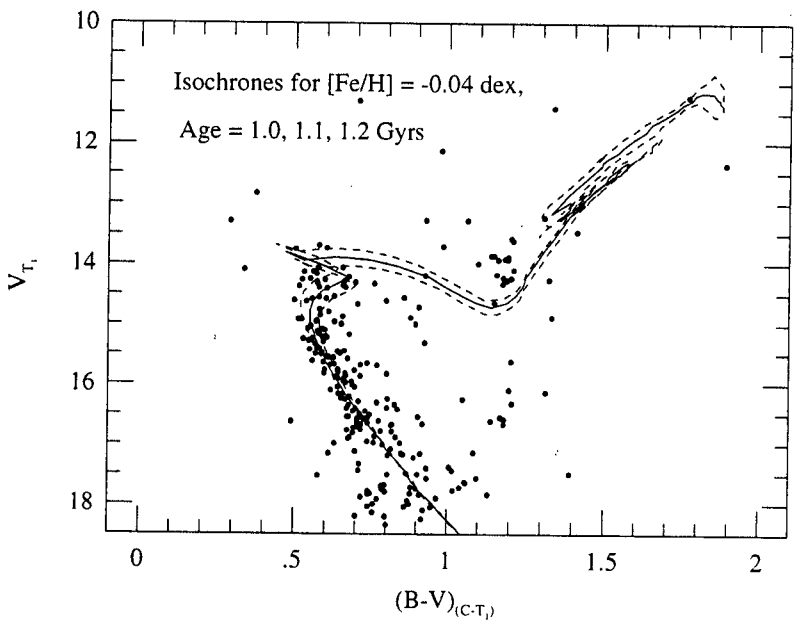

Fig. 6 Isochrone fits for NGC 1245 in the $V-(B-V)$ color-magnitude diagram converted from $T_1-(C-T_1)$ color-magnitude diagram. The solid and dashed lines represent the theoretical isochrones based on the convective overshooting models for the ages of 1.1, 1.0 and 1.2 Gyrs and the metallicity [Fe/H] = –0.04 dex. The isochrones were shifted according to $E(B-V)=0.28$ mag and $(m-M)_V=12.92$.

Table 4. Metallicity estimates using the four color-color diagrams

Metallicity Index	Temperature Index	Mean [Fe/H] (dex)	Mean Error (dex)	Dispersion (dex)
$(C-M)_0$	$(T_1-T_2)_0$	−0.09	±0.03	±0.13
$(C-M)_0$	$(M-T_2)_0$	−0.04	±0.04	±0.15
$(C-T_1)_0$	$(T_1-T_2)_0$	−0.06	±0.03	±0.13
$(C-T_1)_0$	$(M-T_2)_0$	+0.02	±0.03	±0.13
Mean		-0.04 ± 0.05		

Table 5. Comparison with previous studies

References	Method	$E(B-V)$	Distance [kpc]	Age [Gyrs]	[Fe/H] [dex]
Chincarini(1964)	UBV pg.		2.3	0.8	metal-rich
Hagen(1970)	UBV pg.	0.27	2.3		
Janes(1979)	$\delta(U-B)$				+0.06
Lynga(1987)	Lund Catalogue	0.27	2.2	1.1	+0.14
Pandey *et al.*(1989)	Integrated parameter			1.1	
Carraro & Patat(1994)	BV CCD	0.26	3.0	0.8	
This study	Washington CCD	0.28±0.03	2.5±0.2	1.1± 0.1	−0.04±0.16

(Lynga 1987). If they adopt our estimate for the metallicity, they would obtain a smaller value for the distance and a larger value for the reddening compared with what they obtained. They also obtained a value of the age, $t = 7.0 \times 10^8$ yrs using the value for ΔV of 0.40 mag. ΔV was defined as the V magnitude difference between the red giant clump and the main sequence turn-off (0.25 mag below the brightest part in the CMD) by Carraro & Chiosi (1994). Figure 1 in Carraro & Chiosi (1994) shows an indication that the slope of the age–Δ relation is decreasing for the low value of ΔV (= 1–1.5). The youngest cluster used for the calibration of the age – ΔV relation by Carraro & Chiosi (1994) is NGC 752 which has an age 1.5 Gyrs and $\Delta = 1.0$. Carraro & Patat's age estimate for NGC 1245 is based on the extrapolation of the calibration for the age – ΔV relation given by Carraro & Chiosi (see their Fig. 1) so that it may be a underestimate. Finally our estimate for the distance is intermediate among the previous estimates.

V. DISCUSSION

(a) Differential Reddening

Carraro & Patat(1994) suggested that the mean differential reddening is increasing southward in NGC 1245 with a rate of of $d(B-V)/dR = 0.04$ mag/arcmin. We have also examined the differential reddening of NGC 1245, by inspecting the color variation of our photometry, as was done by Carraro & Patat (1994). Figure 7 displays the $(B-V)_{(C-T_1)}$ color distribution of the stars with in the range of $14.0 < V_{T_1} < 16.5$ mag and $0.5 < (B-V)_{(C-T_1)} < 0.9$ which are common among this study, Chincarini (1964) and Carraro & Patat (1994). Most of these stars are main sequence stars. Figure 7 shows the followings. (a) Our data shows that the mean colors are increasing northward with a rate of of $d(B-V)/dR = 0.033 \pm 0.016$ mag/arcmin, indicating that the mean differential reddening is increasing northward in NGC 1245. The magnitude of the changing rate in this study is similar to that given by Carraro & Patat, but the changing direction is the opposite to the Carraro & Patat's result as described above. (b) On the other hand, our data show that the mean colors of this study change little along the east-west direction (with a rate of $d(B-V)/dR = 0.004 \pm 0.006$ man/arcmin). (c) Chincarini's data show the trends similar to our results,

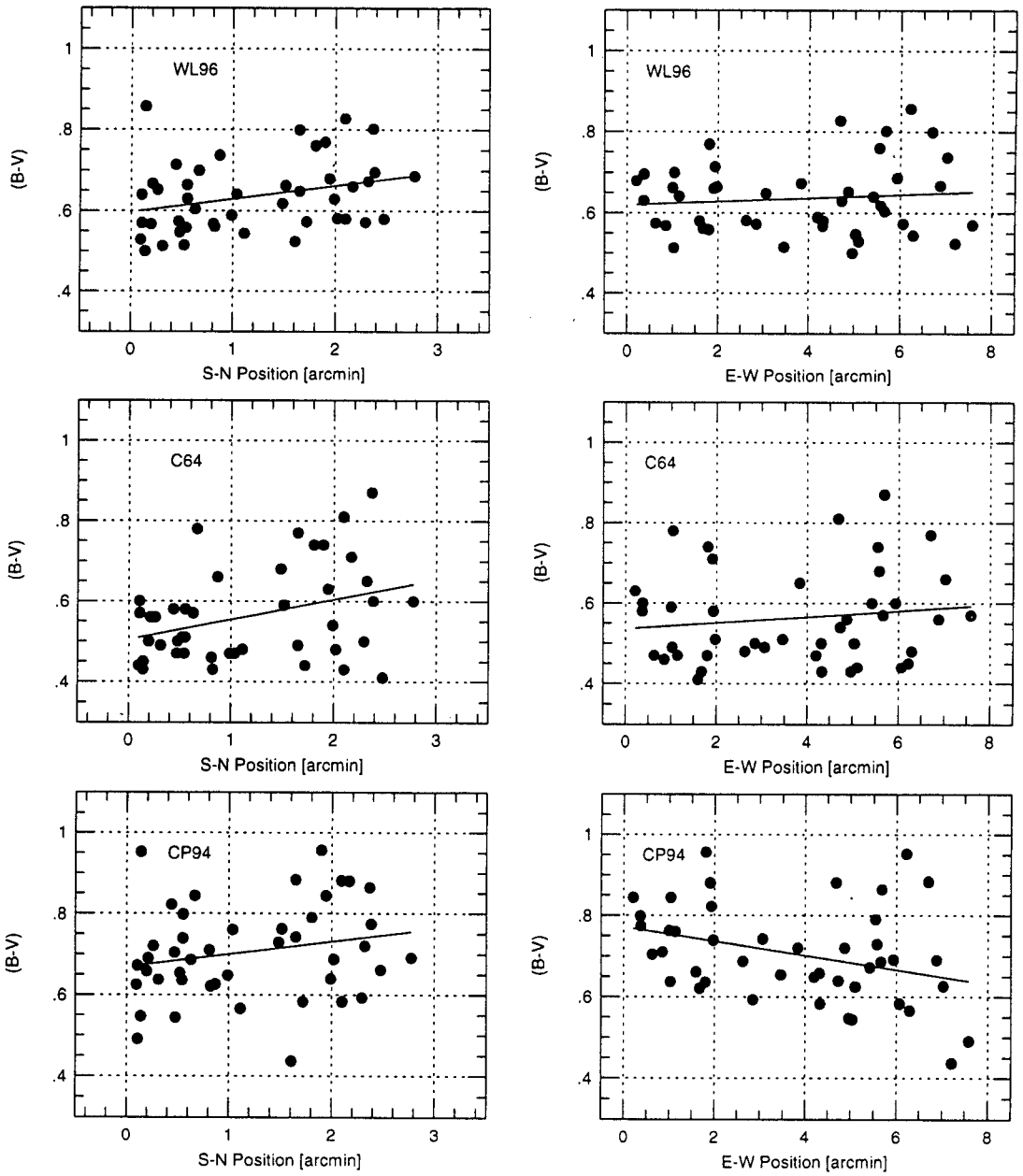

Fig. 7 $(B-V)_{(C-T_1)}$ color distributions of the bright stars in NGC 1245 common among this study, Chincarini (1964) and Carraro & Patat (1994) along the south-north direction (left panels) and east-west direction (right panels). The solid lines in each diagram represent the linear fits.

but with much large scatters. (d) Carraro & Patat's data show a trend along the south-north direction similar to our result, but a different trend along the east-west direction compared with ours. Their mean colors increase eastward. Their colors show larger scatters than ours. The changing direction along the south-north direction shown by the stars common between this and Carraro & Patat's is the opposite to that suggested by Carraro & Patat (1994). Note that this result is based on only the stars common between this study and Carraro & Patat's, while the conclusion on the differential reddening given by Carraro & Patat is based on the stars in the central fields of their study.

We have investigated the reasons for the opposite conclusions of this study and Carraro & Patat as follows. We have plotted in Figure 8 the $(B-V)$ color difference (ours minus Carraro & Patat's) distributions of the bright stars in NGC 1245 common between this study and Carraro & Patat's along the south-north direction and

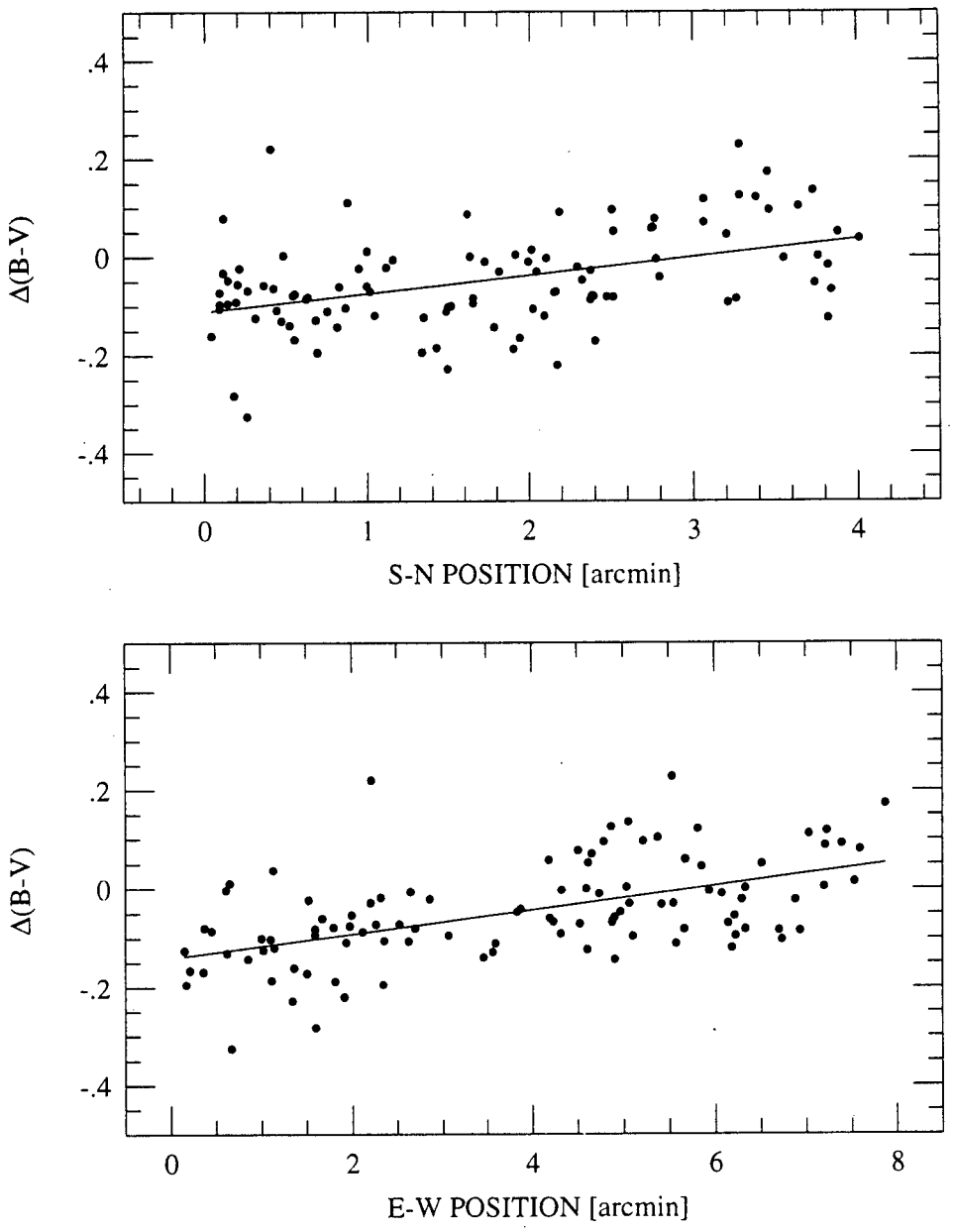

Fig. 8 $(B - V)$ color difference distributions of the bright stars in NGC 1245 common among this study and Carraro & Patat (1994) along the south-north direction (upper panel) and east-west direction (lower panel). The solid lines in each diagram represent the linear fits.

east-west direction. Figure 8 shows that the mean differences increase northward and westward with the rates of $d\Delta(B - V) = 0.037 \pm 0.008$ and 0.024 ± 0.004 mag/arcmin, respectively. This indicates either that the mean colors of Carraro & Patat are systematically redder southward and eastward than those of this study or the opposite. This result explains the reasons for the differences between our results and Carraro & Patat's on the direction of the differential reddening.

We suspect that the systematic color differences between the two studies may be due to some calibration problems in Carraro & Patat's photometry, because their photometry is based on combing seven small fields so that there might have been small photometric differences among the fields. This reasoning is also supported by the fact that the CMDs of each field in their study (their Figure 4) show a morphology of the red giant clump similar to ours,

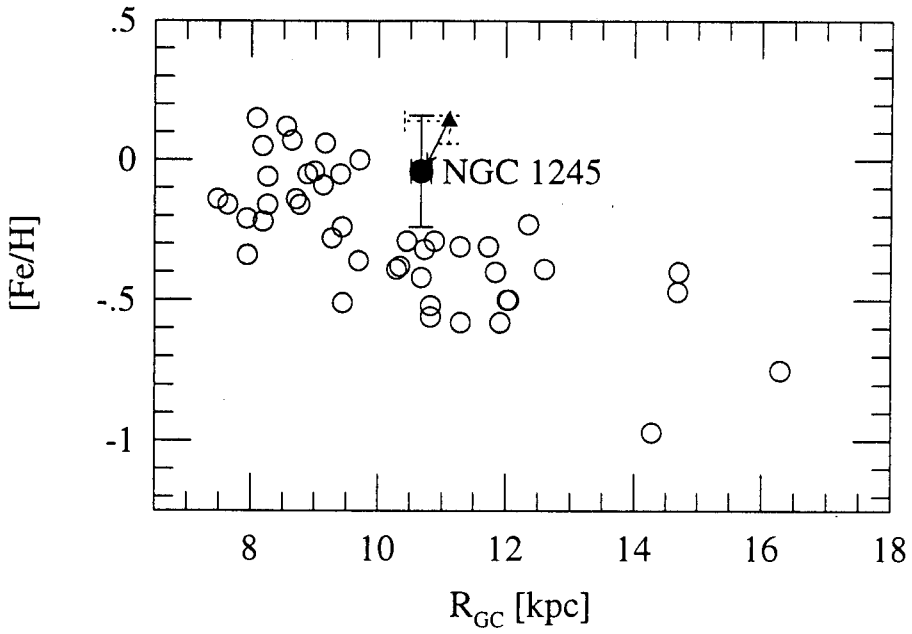

Fig. 9 Radial metallicity gradient of the old open clusters. The open circles represent the old open clusters compiled by Friel (1995) and updated by Lee *et al.*(1996) and by Lee (1997). The ranges of previous estimates of R_{GC} and [Fe/H] of NGC 1245 are marked by the dotted error bars and our estimates for NGC 1245 are represented by the filled circle. The filled triangle represents the metallicity value for NGC 1245 given by Lynga (1987).

while the CMD of their combined photometry show a red giant clump which is much wider in colors than ours and Chincarini's, as shown in Figure 3. Further study of NGC 1245 based on wide field imaging with a large-format CCD is needed to resolve this problem clearly.

(b) The Radial Metallicity Gradient of the Old Open Clusters

As described in Sec. I, previous studies suggested that the metallicity of NGC 1245 is much higher than the value expected at the distance of this cluster from the radial metallicity gradient of the old open clusters. We have estimated the metallicity and galactocentric distance of NGC 1245, [Fe/H] $= -0.4 \pm 0.16$ dex, and $R_{GC} = 10.7 \pm 0.2$ kpc, in the previous sections. Here we use these results to resolve the intriguing problem addressed in Sec. I.

Figure 9 illustrates the radial metallicity gradient of the old open clusters summarized in Friel (1995) and the position of NGC 1245 we have obtained in this study. The data for two old open clusters, Tombaugh 2 and AM-2, are updated using the results given by Lee *et al.*(1996) and Lee (1997). The mean metallicity decreases outward with a slope of Δ[Fe/H]$/R_{GC} = -0.095 \pm 0.017$ dex/kpc (Friel 1995). Figure 9 shows that the position of NGC 1245 is marginally consistent with the metallicity gradient of other old open clusters. From this result we may conclude that NGC 1245 is not abnormally metal-rich and that the previous estimates for the metallicity may be overestimates.

VI. SUMMARY AND CONCLUSIONS

We have presented Washington CCD photometry of ≈260 stars in the central 8′.0 × 4′.3 region of NGC 1245. The primary results are summarized below.

1. The color-magnitude diagram shows a broad main sequence the top of which is located at $T_1 \approx 13.8$ mag and $(C - T_1) \approx 1.1$ (corresponding to $V \approx 14.1$ and $(B - V) \approx 0.6$), and the red giant clump at $T_1 \approx 13.5$ mag and $(C - T_1) \approx 2.3$ (corresponding to $V \approx 14.1$ and $(B - V) \approx 1.2$).

2. The reddening of NGC 1245 is estimated to be $E(B-V) = 0.28 \pm 0.03$.
3. The mean metallicity of NGC 1245 is estimated using the color-color diagram, to be [Fe/H] $= -0.04 \pm 0.16$ dex. This value is lower than the previous estimates, and is consistent with the radial metallicity gradient of the other old open clusters. NGC 1245 is not abnormally metal-rich.
4. The age of NGC 1245 is estimated to be $t = 1.1 \pm 0.1$ Gyrs, using the theoretical isochrones based on the convective overshooting models.
5. The distance of NGC 1245 is determined to be $d = 2.5 \pm 0.2$ kpc (the corresponding galactocentric distance is $R_{GC} = 10.7$ kpc.
6. We have found that there is a systematic differential reddening of $dE(B-V)/dR = 0.033 \pm 0.016$ mag/arcmin increasing northward, while the systematic differential reddening is negligible along the east-west direction.

We thank the staffs of the Sobaeksan Observatory for their support during the observing runs. This research is supported in part by the Ministry of Education, Basic Science Research Institute grant No. BSRI-95-5411, and the Korea Science and Engineering Foundation grant No. 95-0702-01-01-3.

REFERENCES

Bertelli, G., Bressan, A., Chiosi, C., Fagotto, F. & Nasi, E. 1994, A&AS, 106, 275
Canterna, R. 1976, AJ, 81, 228
Carraro, G., & Chiosi, C. 1994, A&A, 287, 761
Carraro, G., & Patat, F. 1994, A&A, 289, 397
Chincarini, G., 1964, Mem. S. A. It., Vol. 35, 2
Friel, E. D. 1995, ARA&A, 33, 381
Geisler, D. 1990, PASP, 102, 344
Geisler, D. 1996, AJ, 111, 480
Geisler, D., Claria, J. J., & Minniti, D. 1991, AJ, 102, 1836
Hagen, G. L. 1970, Pub. David Dunlop Obs., 4, 1
Harris, H., & Canterna, R. 1979, AJ, 84, 1750
Hoag, A. A., Johnson, H. L., Iriarte, B., Mitchell, R. I., Hallam, K. L., & Sharpless, S. 1961, Pub. Naval Obs., Vol. 17, part 7
Janes, K. A. 1979, ApJS, 39, 135
Lee, M. G. 1997, AJ, in press (February issue)
Lee, M. G., Wee, S.-O., & Geisler, D. 1996, in preparation
Lynga, G. 1987, Catalogue of Open Cluster Data
Pandey, A. K., Bhatt, B. C., & Mahra, H. S. 1989, MNRAS, 236, 263